WEBSTERS HORN EQUATION FOR THE RYDBERG SERIES

BY

MATTEO HOCH

THESIS

Submitted in partial fulfillment of the requirements
for the degree of Bachelor of Science in Electrical and Computer Engineering
in the Undergraduate College of the
University of Illinois at Urbana-Champaign, 2016

Urbana, Illinois

Adviser:

Jont Allen

ABSTRACT

In this senior thesis, we explore a wave equation for the energy level spectrum of the electrons of hydrogen in terms of Webster's horn equation instead of the Bohr's radial orbiting model. We seek to derive the area function of Webster's horn equation by matching it to the Rydberg series for hydrogen's electrons. First we derive the dispersion relation for the Rydberg series. Then we utilize that dispersion relation to find a complex analytic impedance function. In our derivation we develop an inverse technique that takes the hydrogen spectrum and yields a closed-form area function of a horn. From this we find a fixed length horn with an closed-form area function to be incompatible with the Rydberg series. Then we start the investigation of a different inverse technique from D. C. Youla which states that given the reflectance and a few other parameters we can completely determine a horn an area function. This addition is still in progress.

Keywords: horn, Rydberg series, Schrödinger equation, Bohr model, energy levels

TABLE OF CONTENTS

CHAPTER 1

INTRODUCTION

Schrödinger's equation was conceived to give a wave equation for the energy levels of hydrogen when Bohr's radial orbiting model [Boh13, p. 8] was found to be flawed[1]. Schrödinger's derivation applied the de Broglie matter-wave relations in a heuristic manner to find a wave equation that successfully predicted hydrogen's energy levels. In this thesis we outline a procedure for deriving a wave equation for the energy levels of hydrogen using a waveguide from acoustics, Webster's horn equation [Web19]. Remarkably, Webster's horn equation is already in the form of the one-dimensional Schrödinger equation [Sal46].

1.1 Dispersion of the Hydrogen Atom

The Rydberg series can be used to compute the emitted wavelength given by any *hydrogen-like*[2] atom's electron transition $m \rightarrow n$ from a higher energy level, m, to a lower energy level, n. Figure 1.1 illustrates this model. The equation for Fig. 1.1 is given by

$$\frac{1}{\lambda} = Z^2 R_H (\frac{1}{n^2} - \frac{1}{m^2}), \tag{1.1}$$

where R_h is Rydberg's constant, Z is the number of protons in the nucleus, n and m are integers, and λ is the emitted wavelength. When n is fixed to some constant, we arrive at the different series discovered independently by their namesakes e.g. $n = 1$

[1] An electron orbiting a nucleus should give off radiation due to its charge [Che, p. 32].

[2] Any nucleus with just one electron is a hydrogen-like atom.

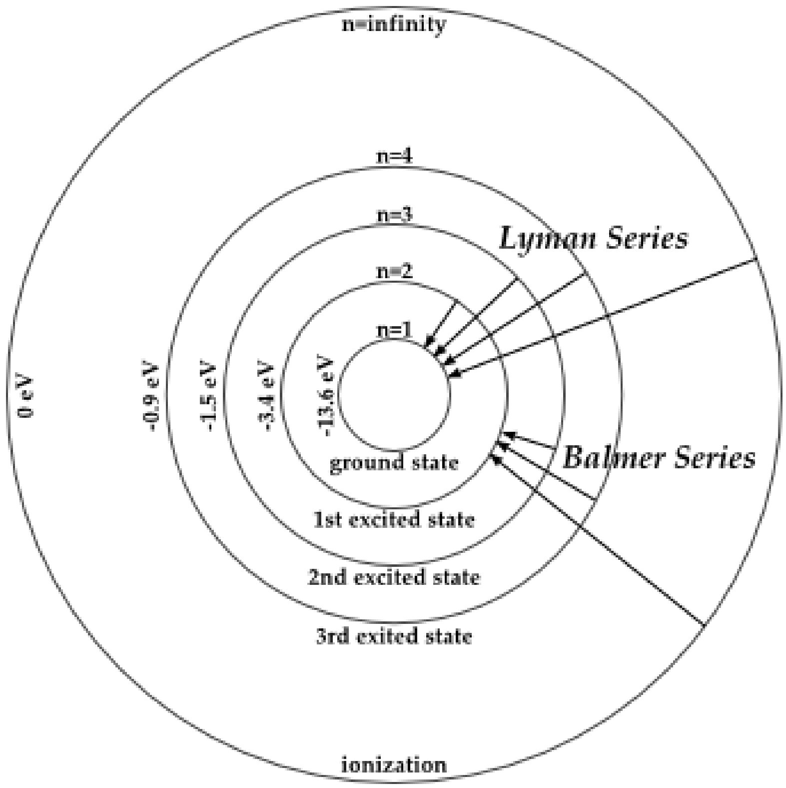

Figure 1.1: A picture of hydrogen's energy transitions from UNL [atUoNL]. The energy level n represents the electron transition's terminal state and the units are given in energy, eV, where $E = h\frac{c}{\lambda}$ from the de Broglie relations. The energy is negative because this electron is viewed as a *trapped* electron.

Ly(man), $n = 2$ Ba(lmer), and $n = 3$ Pa(schen). Figure 1.2 shows the wavelength for the different series of hydrogen, $Z = 1$.

The Rydberg series has discrete modes and has the unique property of a cumulation point for the bound electron. This is also called the *ionization energy.* To investigate this further, we can plot the Rydberg series *dispersion relation* which is a function of the *wavenumber* $k = \varphi(\omega)$ for a wave solution of the form e^{-jkx} where x is distance. The *group delay*, τ, is given by $\tau(\omega) = -\frac{\partial\varphi}{\partial\omega}$. Figure 1.3[3] shows the modes becoming infinitely close together while having infinite delay at the cut-off frequency f_c. This

[3] In Chapter 4 we derive this dispersion relation for the Rydberg series and go into more detail.

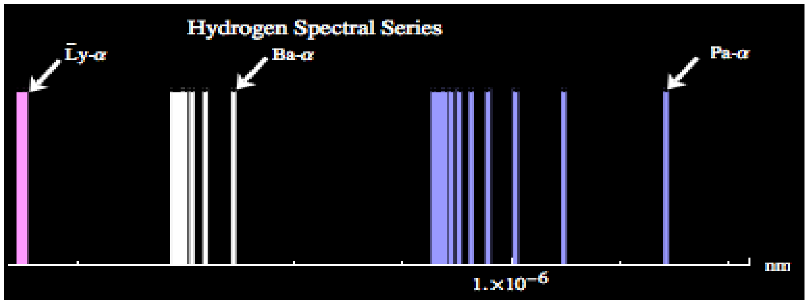

Figure 1.2: Plot of spectral lines of hydrogen as a function of the wavelength from [Ram]. Note the accumulation point at the lowest wavelength of each series. Because the relation between frequency and wavelength ($f\lambda = c$), the frequency is related to the reciprocal of the wavelength. This means that in frequency, the accumulation point is approached from below, reaching an upper cut-off frequency f_c.

implies that the electron is slowing down, to zero, as it approaches the ionization energy.

The cumulation point in Fig. 1.3 is a phenomena so bizarre that Arnold Sommerfeld commented

> This equation reduces to a simple mathematical formula the enigma of the spectral lines, with their finite cumulation point, the behavior of which differs so fundamentally from that of all mechanical systems [Som49].

Sommerfeld goes on to say that the success of the Schrödinger equation is rooted in its analytic model for explaining the cumulation point of the transitions of an electron of hydrogen [Som49].

1.2 Outline

In this thesis we outline a procedure to find a complex analytic impedance function in order to find Webster's horn area function for hydrogen's spectrum. Webster's

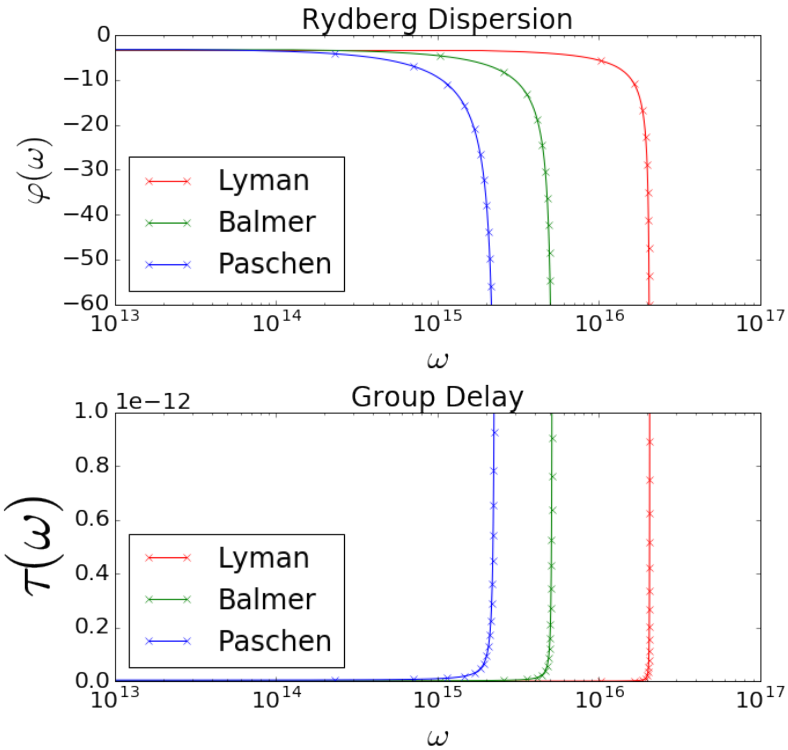

Figure 1.3: The markers are every $2\pi m + \pi$. Note the asymptotic behavior causing a limit to the maximum frequency of the series. This is to be expected since $lim_{m\to\infty}\omega = 2\pi c R_H \left(\frac{1}{n^2}\right)$. We have verified these solutions with the expected spectral limit of the respective series. Higher n gives modes that have a much larger group delay and therefore a lower cutoff frequency.

horn equation is given by[4]

$$\frac{1}{A(x)}\partial_x(A(x)\frac{\partial P}{\partial x}) = \frac{1}{c^2}\frac{\partial^2 P}{\partial t^2} \tag{1.2}$$

where $A(x)$ is the area function of a horn, x is the distance from the "throat" of the horn, c is the wave speed, and P is the average pressure along a wavefront which can be dependent on (x, t) or (x, ω). A plot showing the iso-pressure contours of P by dotted lines is given in Fig. 1.4.

[4]See the appendix for a full derivation.

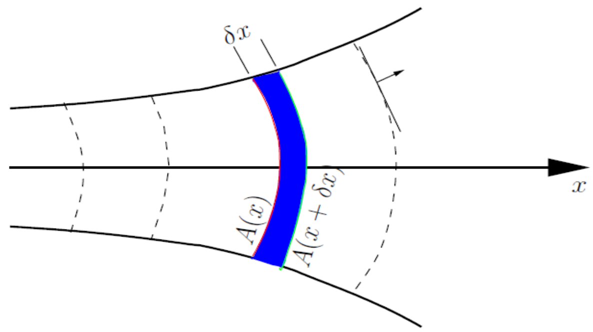

Figure 1.4

The motivation for this work comes from the hydrogen atom electron behaving much more like a waveguide near the cutoff frequency than an electron in orbit as in the Bohr model [Boh13]. Also, Webster's horn equation is equivalent to the one-dimensional Schrödinger equation [Sal46]. In the case of Schrödinger's solution of the hydrogen atom, the radial component is given by [Jon]

$$-\frac{\hbar^2}{2m}\left(\frac{1}{r^2}\frac{\partial}{\partial r}(r^2\frac{\partial}{\partial r}) + V(r)\right)\Psi(r) = \hat{E}\Psi(r). \tag{1.3}$$

where $V(r) = \frac{-e^2}{4\pi\epsilon_0 R^3 r}$ which is known as the *Coulomb potential.* Equation 1.3 is close to Webster's horn equation for the 3D conical horn. The 3D conical horn is given by $A(x) = A_0(x + r_0)^2$ where A_0 is a constant and r_0 gives the radius at the horn's throat [All]. Webster's horn equation becomes

$$\left(\frac{1}{r^2}\frac{\partial}{\partial r}(r^2\frac{\partial P}{\partial r})\right) = \frac{1}{c^2}\frac{\partial^2 P}{\partial t^2}, \tag{1.4}$$

which has equivalent spatial derivatives to Eq. 1.3 with the parameter x changed to r but does not have the potential term, $V(r)$, or the same energy operator $\hat{E}$.

In this thesis, we show the existence of a complex analytic impedance function that explains the eigenmodes of the electron of the hydrogen atom. We highlight the result of Youla which demonstrates that given the impedance and a few other parameters, the area function[5] can be recovered [You64].

In Chapter 3 we give examples of Webster's horn equation through a transmission line analogy [All] and investigate its behavior for the uniform horn and the exponential horn. In the end of the chapter, we introduce an inverse technique for a fixed length horn. Chapter 4 introduces the Rydberg series and we derive its dispersion relation, reflectance, and impedance. In the end of Chapter 4 we find our main result by deriving a complex analytic impedance function, Eq. 4.18. In Chapter 5 we apply our closed-form quadratic inverse technique and find that a fixed length horn Webster's horn yields an unsatisfactory closed-form area function.

After discovering this unsatisfactory area function, we start working through an inverse technique from Youla [You64] that guarantees finding an iterative approximation for the area function from the Rydberg reflectance we derived earlier. This work is still in progress and we mention the next steps in our conclusion.

[5] He uses the term log-line taper in the cited paper

CHAPTER 2

LITERATURE REVIEW

Much of the seminal work on the formulation of the horn is well known in acoustics and the traditional formulation is discussed in many papers and books [Mor48], [Sha70], [Pie81]. It is frequently stated that the Webster horn equation [Web19] is an approximation that only applies to low frequencies, because it is assumed that the area function is the cross-sectional area [Mor48], [Ols47], [Pie81]. A derivation using an iso-phase surface for $A(x)$ has been provided by Allen [All]. A paper by Berners and Smith makes this argument as well [BSI94].

This thesis is started from the work of Allen [All] presented in ECE 493 in Spring 2015 and involves transmission line analogies to Webster's horn equation. There are related papers using ABCD transmission line matrices for Webster's horn equation [Kol], [DC12].

We seek to find a waveguide using Webster's horn equation's area function applied to the Rydberg series for hydrogen, of which the phenomena is notably "[a system whose] behavior differs so fundamentally from that of all mechanical systems" [Som49]. The prediction by Schrödinger for the spectral lines of hydrogen including angular effects was instrumental in giving credit to Schrödinger's equation and the movement away from Sommerfeld and Bohr [Boh13]. The paper by Berner and Smith [BSI94] and the paper of Vincent Salmon [Sal46] make mention of the compatibility of Webster's horn equation and 1D particle scattering by Schrödinger's equation, but this does not hold for scattering from a Coulomb potential, as in the case of the hydrogen atom. D. C. Youla, (1961), finds that given the reflectance of a wave terminated by an arbitrary load impedance it is always possible to find the area function [You64]. We point to his results as a solution to discovering an iterative solution for the area equation for Hydrogen's energy levels.

CHAPTER 3

WEBSTER'S HORN EQUATION

First we go through a transmission line analogy of Webster's horn equation in the general case mirroring the paper by Allen [All] but with a different $\mathcal{P}^{\pm}$ in the derivation. Then we proceed to derive the reflection coefficients, transmission matrix, impedance matrix, and modes of the uniform horn and exponential horn as an exercise to prepare us for the Rydberg series. In Section 3.4 we introduce a closed form inverse method for Webster's horn for use later with the Rydberg series.

3.1 General Case

The Webster's horn equation is given by[1]

$$\frac{\partial^2 P}{\partial x^2} + \frac{1}{A(x)}\frac{\partial A(x)}{\partial x}P(x) = \frac{1}{c^2}\frac{\partial^2 P}{\partial t^2}. \tag{3.1}$$

where c is the acoustic wave speed, $c = \sqrt{\frac{\rho_0}{\eta_0 P_0}}$ as shown by the propagation function

$$\kappa(s) \equiv \sqrt{\mathcal{L}(s,x)\mathcal{Y}(s,x)} = \sqrt{\frac{s\rho_0}{A(x)}\frac{sA(x)}{\eta_0 P_0}} = \frac{s}{c} \tag{3.2}$$

where κ is the complex wavenumber of $Pe^{\kappa(s)}$, $\mathcal{L}$ is the *per-unit-length-impedance*, and $\mathcal{Y}$ is the *per-unit-length-admittance*.

ABCD Transmission matrix: The transmission matrix gives the solution of a

[1]For a full derivation, see the appendix.

horn having finite length, L, and may be expressed as the following two-port matrix relating the pressure and volume velocity at the input and output ports of the horn ($x = 0$ and $x = L$)

$$\begin{bmatrix} \mathcal{P}_0 \\ \mathcal{V}_0 \end{bmatrix} = \begin{bmatrix} \mathcal{A}(s) & \mathcal{B}(s) \\ \mathcal{C}(s) & \mathcal{D}(s) \end{bmatrix} \begin{bmatrix} \mathcal{P}_L \\ -\mathcal{V}_L \end{bmatrix}. \tag{3.3}$$

By definition, the output velocity $\mathcal{V}_L$ of an ABCD matrix is *out* of the port hence the negative sign [All]. The system is reversible when $\mathcal{A} = \mathcal{D}$ and reciprocal when the determinant of the transmission matrix $\triangle_T = 1$. For Webster's horn equation the horn must be reciprocal [Val64].

Boundary Conditions: The pressure and velocity at any point x can be written in terms of a superposition of the inbound and reflected waves $\mathcal{P}^+(x, s)$ and $\mathcal{P}^-(x, s)$[2]

$$\begin{bmatrix} \mathcal{P}(x) \\ \mathcal{V}(x) \end{bmatrix} = \begin{bmatrix} \mathcal{P}^+(x) & \mathcal{P}^-(x) \\ Y^+_{rad}\mathcal{P}^+(x) & -Y^-_{rad}\mathcal{P}^-(x) \end{bmatrix} \begin{bmatrix} \alpha \\ \beta \end{bmatrix}. \tag{3.4}$$

Coefficients $\alpha(\omega)$ and $\beta(\omega)$, which depend only on ω and not x, are determined by the boundary conditions at $x = L$.

Transmission Matrix: To find the transmission matrix from Eq. 3.4 we can solve for α and β taking advantage of the fact that they have no x dependence. To make these computations more compact we introduce new notation and normalization. $\mathcal{P}_0^\pm = \mathcal{P}^\pm(x = 0)$ and the determinant of the above matrix evaluated at $x = L$ as $\triangle_L$. Also we normalize $\mathcal{P}_0^+ = 1$ and $\mathcal{P}_L^- = 1$ as in

$$\triangle_L = -\mathcal{P}_L^+[Y^+_{rad}(L) + Y^-_{rad}(L)] \tag{3.5}$$

$$\begin{bmatrix} \alpha \\ \beta \end{bmatrix}_L = -\frac{1}{\triangle_L} \begin{bmatrix} Y^-_{rad} & -1 \\ Y^+_{rad}\mathcal{P}_L^+ & \mathcal{P}_L^+ \end{bmatrix} \begin{bmatrix} \mathcal{P}_L \\ -\mathcal{V}_L \end{bmatrix}. \tag{3.6}$$

[2]Here we diverge from Allen's derivation [All] in order to keep the reflection $\Gamma = \frac{\beta}{\alpha}$, [**?** , Eq. 18] instead of his $\Gamma = \frac{\beta}{\alpha e^{\kappa L}}$ caused by his definition $\mathcal{P}_L^-(x) = \mathcal{P}^-(x - L)$ in his superposition matrix.

Now we can substitute this back into Eq. 3.4 evaluated at $x = 0$ to find the transmission matrix

$$\begin{bmatrix} \mathcal{P}_0 \\ \mathcal{V}_0 \end{bmatrix} = -\frac{1}{\triangle_L} \begin{bmatrix} 1 & \mathcal{P}_0^- \\ Y_{rad}^+ & -Y_{rad}^- \mathcal{P}_0^- \end{bmatrix}_0 \begin{bmatrix} Y_{rad}^- & -1 \\ Y_{rad}^+ \mathcal{P}_L^+ & \mathcal{P}_L^+ \end{bmatrix}_L \begin{bmatrix} \mathcal{P}_L \\ -\mathcal{V}_L \end{bmatrix}. \tag{3.7}$$

The subscript to the right of each matrix indicates Y_{rad} is evaluated at $x = 0$ or $x = L$.

Reflectance: The reflectance is given by the ratio of the reflected wave amplitude, β, to the incident wave amplitude, α. The reflectance is given by [All, Eq.18]

$$\Gamma_L(s) \equiv \frac{\beta}{\alpha}. \tag{3.8}$$

The reflectance has a critical role in the theory of horns because it relates the modes of a horn to its area function.

Impedance Matrix: The impedance matrix can be expressed in terms of the ABCD transmission matrix elements

$$\begin{bmatrix} \mathcal{P}_0 \\ \mathcal{P}_L \end{bmatrix} = \frac{1}{\mathcal{C}(s)} \begin{bmatrix} \mathcal{A}(s) & \triangle_T \\ 1 & \mathcal{D}(s) \end{bmatrix} \begin{bmatrix} \mathcal{V}_0 \\ \mathcal{V}_L \end{bmatrix}. \tag{3.9}$$

Note that $\triangle_T = 1$ since the horn must be *reciprocal* [Val64].

3.2 Example of the Uniform Horn

For the case of the uniform horn, the area function becomes $A(x) = A_0$ and Eq. 3.1 reduces to [All]

$$\mathcal{P}_{xx} + \frac{\omega^2}{c^2}\mathcal{P} = 0. \tag{3.10}$$

This leads to the normalized solutions

$$\rho^\pm(x,t) = \delta(t \mp x/c) \leftrightarrow \mathcal{P}^\pm(x) = e^{\mp\kappa x} \tag{3.11}$$

and

$$\mathcal{P}(x) = \alpha(\omega)e^{-\kappa x} + \beta(\omega)e^{\kappa x}. \tag{3.12}$$

First ABCD matrix: Using Eq. 3.12 We have our first ABCD matrix

$$\begin{bmatrix} \mathcal{P}(x) \\ \mathcal{V}(x) \end{bmatrix} = \begin{bmatrix} e^{-\kappa x} & e^{\kappa x} \\ \mathcal{Y}e^{-\kappa x} & -\mathcal{Y}e^{\kappa x} \end{bmatrix} \begin{bmatrix} \alpha \\ \beta \end{bmatrix}. \tag{3.13}$$

Solving for α and β evaluated at $x = L$ gives

$$\begin{bmatrix} \alpha \\ \beta \end{bmatrix}_L = -\frac{1}{2\mathcal{Y}} \begin{bmatrix} -\mathcal{Y}e^{\kappa L} & -e^{\kappa L} \\ -\mathcal{Y}e^{-\kappa L} & e^{-\kappa L} \end{bmatrix} \begin{bmatrix} \mathcal{P}_L \\ \mathcal{V}_L \end{bmatrix} = \frac{1}{2} \begin{bmatrix} e^{\kappa L} & \mathcal{Z}e^{\kappa L} \\ e^{-\kappa L} & -\mathcal{Z}e^{-\kappa L} \end{bmatrix} \begin{bmatrix} \mathcal{P}_L \\ \mathcal{V}_L \end{bmatrix}. \tag{3.14}$$

Evaluating Eq. 3.13 at $x = 0$ and substituting in Eq. 3.14 using $\begin{bmatrix} \alpha \\ \beta \end{bmatrix}_0 = \begin{bmatrix} \alpha \\ \beta \end{bmatrix}_L$ we find our transmission ABCD matrix to be

$$\begin{bmatrix} \mathcal{P}_0 \\ \mathcal{V}_0 \end{bmatrix} = \frac{1}{2} \begin{bmatrix} 1 & 1 \\ \mathcal{Y} & -\mathcal{Y} \end{bmatrix} \begin{bmatrix} e^{\kappa L} & \mathcal{Z}e^{\kappa L} \\ e^{-\kappa L} & -\mathcal{Z}e^{-\kappa L} \end{bmatrix} \begin{bmatrix} \mathcal{P}_L \\ \mathcal{V}_L \end{bmatrix}. \tag{3.15}$$

Multiplying these out gives the final transmission matrix as

$$\begin{bmatrix} \mathcal{P}_0 \\ \mathcal{V}_0 \end{bmatrix} = \begin{bmatrix} \cosh(\kappa L) & \mathcal{Z}\sinh(\kappa L) \\ \mathcal{Y}\sinh(\kappa L) & \cosh(\kappa L) \end{bmatrix} \begin{bmatrix} \mathcal{P}_L \\ \mathcal{V}_L \end{bmatrix}. \tag{3.16}$$

Note that the $\triangle_T = 1$, which is a necessary condition from Morse and Feshbach[3] [Mor48]. Similarly, we can find the impedance matrix as

$$\begin{bmatrix} \mathcal{P}_0 \\ \mathcal{P}_L \end{bmatrix} = \frac{\mathcal{Z}}{\sinh(\kappa L)} \begin{bmatrix} \cosh(\kappa L) & 1 \\ 1 & \cosh(\kappa L) \end{bmatrix} \begin{bmatrix} \mathcal{V}_0 \\ \mathcal{V}_L \end{bmatrix}. \tag{3.17}$$

[3] In [Mor48] they define the wave with coefficient β by $e^{\kappa(x-L)}$. Switching the wave at the load to $e^{\kappa x}$ causes $\triangle_T = 1$.

Reflectance: Plugging in α and β into Eq. 3.8 gives

$$\Gamma_0(s) = \frac{\beta}{\alpha} = \frac{\mathcal{P}_0 - \mathcal{Z}\mathcal{V}_0}{\mathcal{P}_0 + \mathcal{Z}\mathcal{V}_0} \tag{3.18}$$

and

$$\Gamma_L(s) = \frac{\beta}{\alpha} = e^{-2\kappa L}\frac{\mathcal{P}_L - \mathcal{Z}\mathcal{V}_L}{\mathcal{P}_L + \mathcal{Z}\mathcal{V}_L}.^{4} \tag{3.19}$$

Boundary Conditions: We are mainly concerned with horns closed at the source, $x = 0$, and opened at the load, $x = L$. These conditions require $\mathcal{V}_0 = 0$ and $\mathcal{P}_L = 0$. Recalling the impedance matrix general form, Eq. 3.9, we have

$$\begin{bmatrix} \mathcal{P}_0 \\ \mathcal{P}_L \end{bmatrix} = \frac{1}{\sinh(\kappa L)} \begin{bmatrix} \cosh(\kappa L) & 1 \\ 1 & \cosh(\kappa L) \end{bmatrix} \begin{bmatrix} \mathcal{V}_0 \\ \mathcal{V}_L \end{bmatrix}. \tag{3.20}$$

Plugging in the constraints into Eq. 3.20 we find the two equations

$$\mathcal{P}_0 = \operatorname{csch}(\kappa L)\mathcal{V}_L \tag{3.21}$$

$$0 = \coth(\kappa L)\mathcal{V}_L. \tag{3.22}$$

We can solve the bottom equation to find the zeros of $\mathcal{V}_L$ given by

$$\kappa L = j(2\pi n + \pi). \tag{3.23}$$

Equation 3.23 holds for all horns closed at the source and open at the load.

Dispersion Relation: For the uniform horn Eq. 3.10 gives $k(\omega) = \mp\frac{\omega}{c}$. This is known as the *dispersion relation* and is shown in Fig. 3.1.

This concludes our investigation of the uniform horn. Fig. 3.1 demonstrates that the uniform horn allows a frequency range that extends from 0 to infinity. In the

[4] Here we differ from [All] because we have written the load equation as $e^{\kappa x}$ instead of $e^{\kappa(x-L)}$. Switching this recovers the factor of $e^{-2\kappa L}$ in our equation.

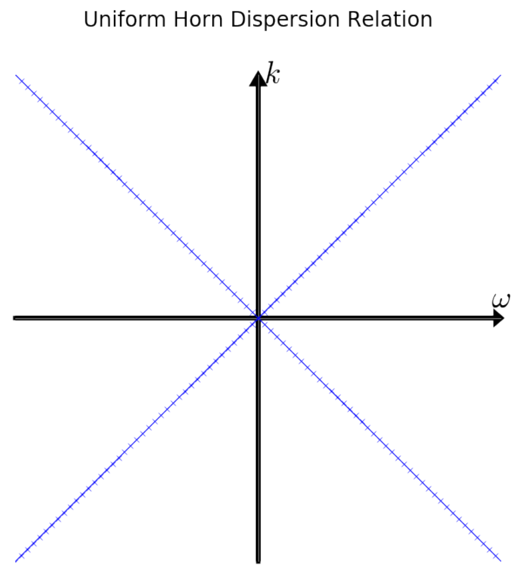

Figure 3.1: Plot of $k(\omega)$ with markers $2\pi n + \pi$ as determined in Eq. 3.23.

next section we look at a horn with a *cutoff* frequency, the exponential horn.

3.3 Exponential Horn

The exponential horn is given by $A(x) = A_0 e^{2mx}$ where m is known as the flare constant. In this case Webster's horn equation becomes [All]

$$\mathcal{P}_{xx} + 2m\mathcal{P}_x = \kappa^2 \mathcal{P}. \tag{3.24}$$

The *characteristic roots* given by solving eq(3.13) for $\mathcal{P}(s) = P(s)e^{-\kappa(s)x}$ are $\kappa_\pm(s) = m \pm \sqrt{m^2 + \kappa^2}$. Now we have inbound and outbound waves given by

$$\mathcal{P}^\pm(x) = e^{-mx} e^{\mp\sqrt{m^2+\kappa^2}x}. \tag{3.25}$$

First ABCD Matrix: Again we go through the procedure in the uniform horn. We find

$$\begin{bmatrix} \mathcal{P}(x) \\ \mathcal{V}(x) \end{bmatrix} = e^{-mx} \begin{bmatrix} e^{-j\sqrt{m^2+\kappa^2}x} & e^{j\sqrt{m^2+\kappa^2}x} \\ Y_{rad}^{+} e^{-j\sqrt{m^2+\kappa^2}x} & -Y_{rad}^{-} e^{j\sqrt{m^2+\kappa^2}x} \end{bmatrix} \begin{bmatrix} \alpha \\ \beta \end{bmatrix} \tag{3.26}$$

Solving for the inverse and letting $k = \sqrt{m^2+\kappa^2}$ we find the term before the matrix, e^{-mx}, is canceled out. This gives the reflection coefficients

$$\begin{bmatrix} \alpha \\ \beta \end{bmatrix} = \frac{s}{2\mathcal{Y}\sqrt{(mc)^2+s^2}} \begin{bmatrix} Y_{rad}^{-} e^{jkx} & e^{jkx} \\ Y_{rad}^{+} e^{-jkx} & -e^{-jkx} \end{bmatrix} \begin{bmatrix} \mathcal{P}(x) \\ \mathcal{V}(x) \end{bmatrix}. \tag{3.27}$$

where $Y_{rad}^{\pm} = (x_0, s) = \frac{\mathcal{Y}}{s}\left(mc \mp \sqrt{(mc)_{+}^{2}s^2}\right)$.

Boundary Conditions: We repeat the conditions we imposed on the uniform horn: $\mathcal{V}_0 = 0$ and $\mathcal{P}_L = 0$. From the impedance matrix, Eq. 3.9, we have

$$\begin{bmatrix} \mathcal{P}_0 \\ \mathcal{P}_L \end{bmatrix} = \frac{Z_{rad}^{-} - Z_{rad}^{+}}{\sinh(\kappa L)} \begin{bmatrix} \cosh(\kappa L) & 1 \\ 1 & \cosh(\kappa L) \end{bmatrix} \begin{bmatrix} \mathcal{V}_0 \\ \mathcal{V}_L \end{bmatrix}. \tag{3.28}$$

Plugging in the constraints $\mathcal{V}_0 = 0$ and $\mathcal{P}_L = 0$ into Eq. 3.28 we find the two equations:

$$\mathcal{P}_0 = \left(Z_{rad}^{-} - Z_{rad}^{+}\right)\operatorname{csch}(\kappa L)\mathcal{V}_L \tag{3.29}$$

$$0 = \left(Z_{rad}^{-} - Z_{rad}^{+}\right)\coth(\kappa L)\mathcal{V}_L. \tag{3.30}$$

Similarly to Eq. 3.23, we can solve Eq. 3.30 for the non-trivial case of $Z_{rad}^{-} \neq Z_{rad}^{+}$ and find the zeros to be given by

$$\kappa L = j(2\pi n + \pi). \tag{3.31}$$

Dispersion Relation: As in the uniform horn, we can plot the dispersion relation where $\kappa = jk$. This leads to the dispersion relation

$$k(\omega) = \frac{\sqrt{\omega^2 - (mc)^2}}{c}. \tag{3.32}$$

Because $k(\omega)$ is imaginary for $\omega < mc$ and real for $\omega > mc$, $\omega_c = mc$ is known as the *cutoff* frequency. Rewriting Eq. 3.32 in terms of ω_c we have

$$k(\omega) = \frac{\sqrt{\omega^2 - \omega_c^2}}{c} \tag{3.33}$$

and a plot of Eq. 3.33 with the axes reversed is shown below in Fig. 3.2 from [All].

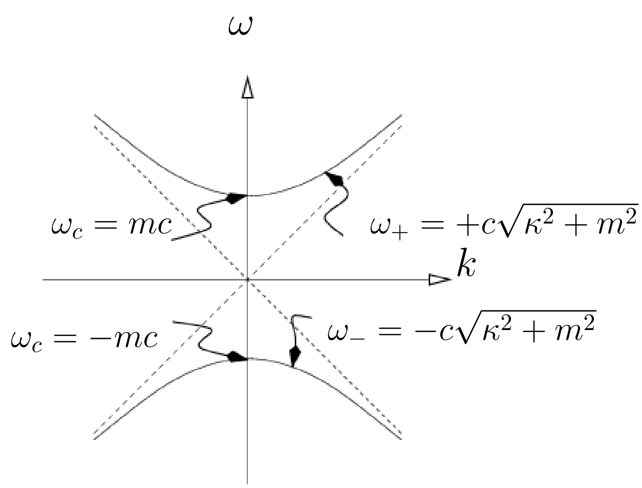

Figure 3.2: This shows the dispersion relation between the frequency and the wave number k for the exponential horn, with wave propagation disallowed below the critical frequency $\omega_c = mc$.

3.4 Quadratic Inverse Technique

In this section we demonstrate the validity of a closed-form inverse technique. We will attempt this later in Section 5.1 to derive a closed-form solution to the area function for the Rydberg series.

Technique Using the boundary conditions from Eq. 3.31 we can solve for the area function given the modes. Defining $Im\{\kappa\}$ through the propagation function or by fitting the boundary conditions $kL = 2\pi n + \pi$ to the transmission matrix we can derive $A(x)$. Here we derive $A(x)$ from the propagation function for the exponential horn

$$\mathcal{P}^{\pm}(x) = e^{-\frac{\omega_c}{c}x} e^{\mp j\sqrt{\omega^2-\omega_c^2}\frac{x}{c}}. \tag{3.34}$$

Solving for κ we have

$$\kappa_{\pm}^2 \mathcal{P} + \frac{1}{A(x)}\frac{\partial A(x)}{\partial x}\kappa_{\pm}\mathcal{P} + \frac{\omega^2}{c^2}\mathcal{P} = 0, \tag{3.35}$$

which can be written as

$$a\kappa_{\pm}^2 + b\kappa_{\pm} + d = 0 \tag{3.36}$$

where a, b, and d are the coefficients of $\mathcal{P}$ and the flare parameter is $m = \frac{\omega_c}{c}$ [All]. For a fixed length, L, the exponential horn becomes $Im(\kappa) = \frac{\sqrt{\omega^2-\omega_c^2}}{c}$. Solving for $A(x)$ we apply the quadratic formula to the imaginary part of the values a, b, d in 3.36

$$Im(\kappa_{\pm}) \equiv k_{\pm} = \pm\frac{\sqrt{\omega^2-\omega_c^2}}{c} = \frac{\sqrt{4ad-b^2}}{2a}. \tag{3.37}$$

Assuming $\mathcal{P}(x) = \mathcal{P}_0 e^{j\omega t - \kappa x}$ and $\omega, A(x)$ have no κ dependence leads to $a = 1, d = \frac{\omega^2}{c^2}$ and then Eq. 3.29 becomes

$$k_{\pm} = \pm\frac{\sqrt{4\frac{\omega^2}{c^2} - b^2}}{2} = \pm\frac{1}{c}\sqrt{\omega^2-\omega_c^2} \tag{3.38}$$

and solving for b gives

$$b = \pm 2\frac{\omega_c}{c} = \frac{1}{A(x)}\frac{\partial A(x)}{\partial x}. \tag{3.39}$$

Finally, solving for $A(x)$ gives

$$\begin{aligned}\frac{\partial A(x)}{\partial x} &= \pm 2\frac{\omega_c}{c}A(x)\\ A(x) &= A_0 e^{\pm 2\frac{\omega_c}{c}} = A_0 e^{2mx},\end{aligned} \tag{3.40}$$

which yields the expected $A(x)$ from Webster's horn equation for the exponential horn Eq. 3.24. In Section 5.1 we attempt this technique for the Rydberg series.

CHAPTER 4

RYDBERG SERIES

Now we introduce the Rydberg formula and develop our transmission line analogy for inverse problem of generating the Webster's horn's area function. We also complete our derivation of Fig. 1.3 in Section 4.2.

4.1 Transmission Line

In this section we derive an equivalent acoustic waveguide for Rydberg systems. We interpret the dispersion relation given by the Rydberg series as a transmission line and look for purely reactive modes given by the load reflectance $\Gamma_L(\omega) = -1$. For all of these derivations we will use the boundary conditions closed at the source and open at the load giving $\varphi(n) = 2\pi n + \pi$ as shown in Eq. 3.31. We have the phase of $\Gamma_L(\omega)$ as

$$\varphi(\omega(n)) = 2\pi n + \pi, . \tag{4.1}$$

The load reflectance is

$$\Gamma_L(\omega) = e^{j\varphi(\omega(n))} \tag{4.2}$$

and the load impedance

$$\mathcal{Z}_L(s) = z_o \frac{1 + \Gamma_L(s)}{1 - \Gamma_L(s)}. \tag{4.3}$$

The formula used for plotting the transmission line variables is derived starting from Eq. 4.1 and Eq. 1.1 for each of the different Rydberg series: Lyman, Balmer, Paschen. We can transform the Rydberg series into ω by taking

$$\frac{1}{\lambda} = R_H \left(\frac{1}{n^2} - \frac{1}{m^2} \right) \tag{4.4}$$

and using $\lambda f = c$ and $\omega = 2\pi f$ we find

$$\omega = 2\pi c R_H \left(\frac{1}{n^2} - \frac{1}{m^2} \right). \tag{4.5}$$

Now we can invert Eq. 4.5 to find $m(\omega)$

$$\begin{aligned} \omega = 2\pi R_H c \left(\frac{1}{n^2} - \frac{1}{m^2} \right) = 2\pi R_H c \left(\frac{\frac{m^2}{n^2} - 1}{m^2} \right) \\ \left(m^2\omega - 2\pi R_H c \frac{m^2}{n^2} \right) \omega = -2\pi R_H c. \end{aligned} \tag{4.6}$$

Solving for m gives

$$m(\omega) = \sqrt{\frac{2\pi R_H c}{\frac{2\pi R_H c}{n^2} - \omega}} \tag{4.7}$$

where m is real. Putting this into Eq. 4.1 gives

$$\varphi(\omega) = \sqrt{\frac{8\pi^3 R_H c}{\frac{2\pi R_H c}{n^2} - \omega}} + \pi, \tag{4.8}$$

where n determines the series we wish to show (e.g. n=1 Lyman, n=2 Balmer, n=3 Paschen).

On the next few pages are plots of the real parts of $\varphi(\omega)$, $\Gamma_L(\omega)$, and $\mathcal{Z}_L(\omega)$ at $\omega_c = \frac{2\pi R_H c}{n^2}$. Note the existence of cumulation point in each series.

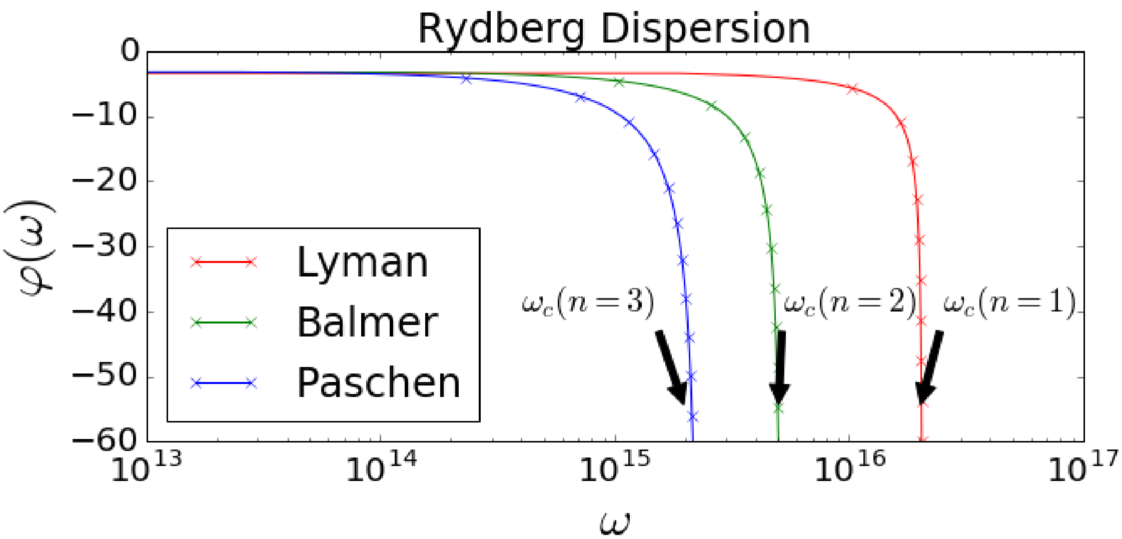

Figure 4.1: Markers every $2\pi m + \pi$. Note the asymptotic behavior causing a limit to the maximum frequency of the series. This is to be expected since $\lim_{m\to\infty}\omega = 2\pi c R\left(\frac{1}{n^2}\right)$. These solutions have been verified with the expected spectral limit of the respective series.

4.2 Rydberg Energy Levels

Using the figures from the prior section as a starting point, we look for the energy levels of hydrogen. To do this we take the limit of the Rydberg series, Eq. 4.5, as m approaches the ionization energy, $m \to \infty$

$$\begin{aligned} \omega(n) &= \lim_{m\to\infty} 2\pi c R_H \left(\frac{1}{n^2} - \frac{1}{m^2}\right) \\ \omega(n) &= \frac{2\pi c R_H}{n^2}. \end{aligned} \tag{4.9}$$

In Bohr's derivation of the Rydberg series for his atomic model [Boh13], he begins by finding E_n[1] and then derives the differences between states m and n for a transition from $m \to n$. By applying de Broglie's relation, $E = \hbar\omega$, we see that taking the limit as $m \to \infty$ for Eq. 4.9 gives the radial energy levels of hydrogen without the

[1]In his Bohr's paper he uses W_τ for E_n.

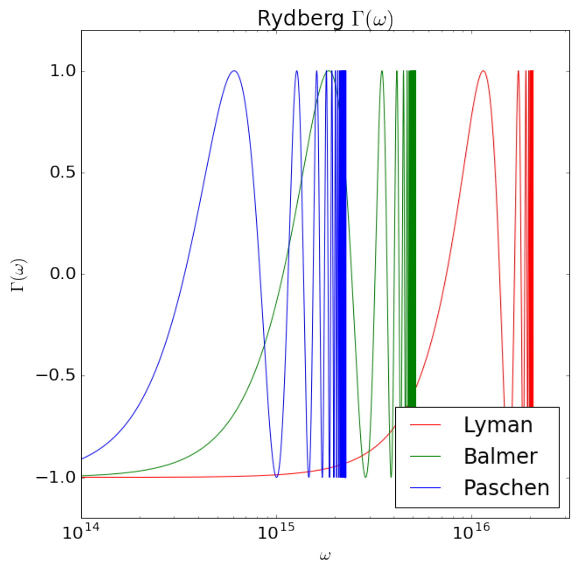

Figure 4.2: $\text{Re}\{\Gamma_L(\omega)\}$ of three Rydberg series

angular component. The energy levels are [Tow10]

$$E_n = -\hbar 2\pi c R_H \frac{1}{n^2} = \frac{-13.6}{n^2} \text{ (eV)} \tag{4.10}$$

where the negative sign denotes that the electron is "trapped" in the potential well of the electron's Coulomb potential [Tow10]. Satisfied with Eq. 4.9, we may find the inverse of $\omega(n)$

$$n(\omega) = \sqrt{\frac{2\pi c R_H}{\omega}}. \tag{4.11}$$

The reflectance phase is then given by

$$\varphi(n) = \pi + 2\pi n. \tag{4.12}$$

Substituting Eq. 4.11 into Eq. 4.12 yields

$$\varphi(\omega) = \pi + \sqrt{\frac{8\pi^3 c R_H}{\omega}}, \tag{4.13}$$

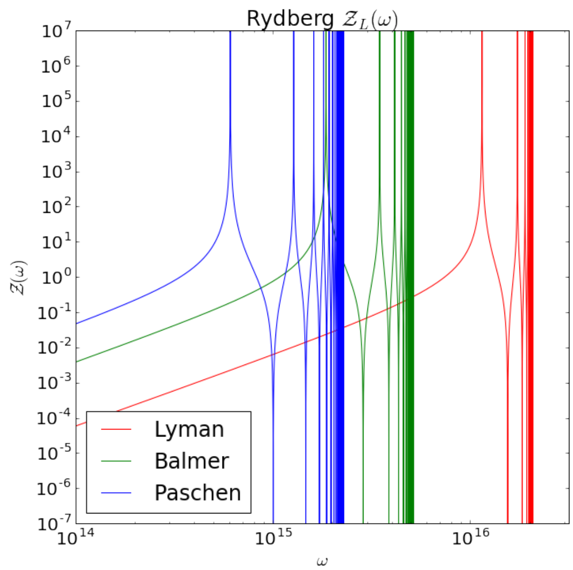

Figure 4.3: Plot of $\mathcal{Z}_L(\omega)$ on log scale. The values are clipped at $\pm 10^7$ to give a good enough picture of the poles and zeros for plotting purposes.

giving the reflectance

$$\Gamma_L(\omega) = e^{-j\varphi(\omega)} = e^{-j\pi} e^{-j\sqrt{\frac{8\pi^3 c R_H}{\omega}}}. \tag{4.14}$$

This gives a similar $\varphi(\omega)$ to the Eq. 4.5 but now the cumulation point is at $\omega = 0$ since

$$\begin{aligned} f_c &= \lim_{n\to\infty} \frac{cR_H}{n^2} \\ f_c &= 0 \end{aligned} \tag{4.15}$$

and the behavior of ω is now reversed because we have let n be free now instead of m. Figure 4.4 shows $\Gamma_L(\omega)$, Eq. 4.14.

Complex Reflectance: In order to find $\Gamma_L(s)$ we first need to write $\Gamma(\omega)$, Eq. 4.14, in terms of $j\omega$ and then s. For compactness we derive $\Gamma_L(s)$ in terms of $\ln(\Gamma_L)$. We

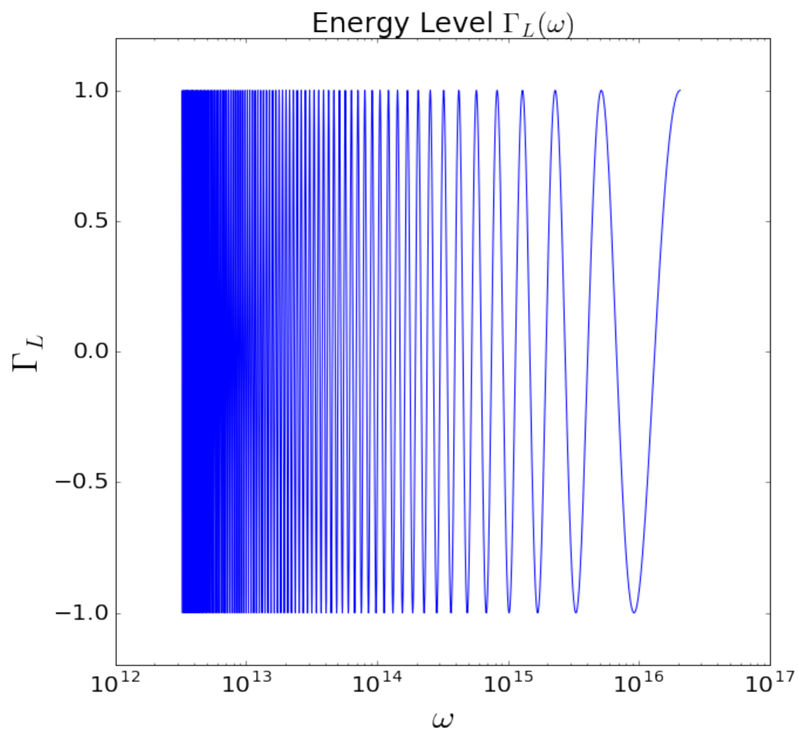

Figure 4.4: As Γ_L approaches the culmination point $\omega = 0$ it takes an infinite amount of modes to get there. This is a plot of the first 80 modes where higher modes corresond to lower ω.

find

$$\ln(\Gamma_L(j\omega)) = -j\pi - j\sqrt{\frac{8\pi^3 cR_H j}{j\omega}} = -j\pi - j\sqrt{8\pi^3 cR_H}\sqrt{\frac{e^{j\frac{\pi}{2}}}{j\omega}}. \tag{4.16}$$

Let $j\omega = s$ to give

$$\begin{aligned} &= -j\pi - j\sqrt{\frac{8\pi^3 cR_H}{j\omega}} e^{j\frac{\pi}{4}} \\ \ln(\Gamma_L(s)) &= -j(\pi + e^{j\frac{\pi}{4}}) - j\sqrt{\frac{8\pi^3 cR_H}{s}}. \end{aligned} \tag{4.17}$$

Finally we have

$$\Gamma_L(s) = e^{-j(\pi + e^{j\frac{\pi}{4}})} e^{-j\sqrt{\frac{8\pi^3 c R_H}{s}}}. \tag{4.18}$$

Eq. 4.18 is plotted in Fig. 4.5.

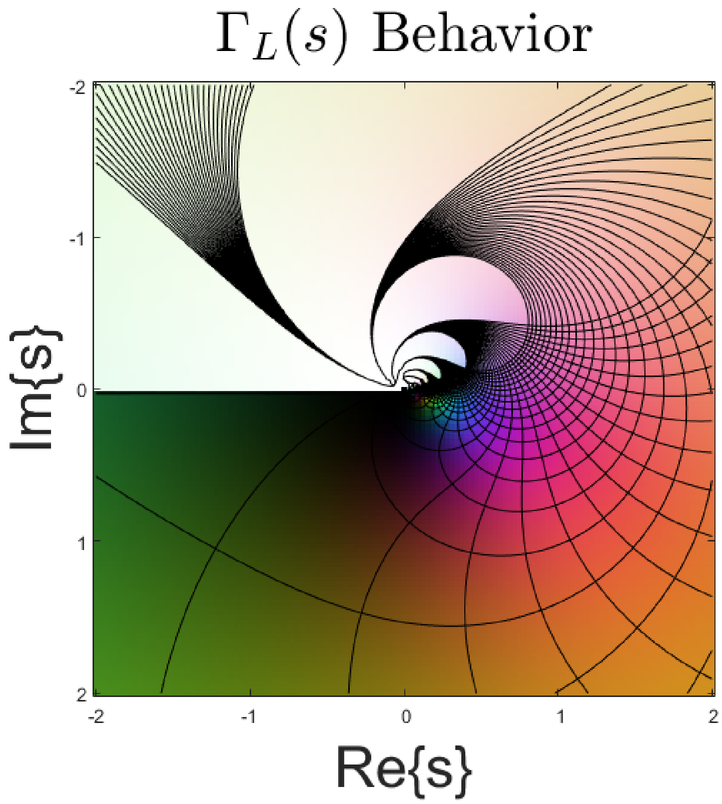

Figure 4.5: $\Gamma_L(s)$ from Eq. 4.18. Plotted with zviz Matlab package. Note the accumulation point when $Im\{s\} = j\omega = 0$.

Figure 4.5 exhibits a cumulation point similar to our plots for the Rydberg series in 4.2 and 4.3. The distinction is that now we have found a complex analytic $\Gamma_L(s)$. Every complex reflectance function is causal since it has an inverse Laplace transform, which is causal $\gamma_L(t) \leftrightarrow \Gamma_L(s)$.

Complex Impedance: Now we can find the complex impedance $\mathcal{Z}(s)$ plugging Eq. 4.18 into Eq. 4.3 as follows:

$$\begin{aligned} \mathcal{Z}_L(s) &= z_o \frac{1+\Gamma_L}{1-\Gamma_L} = z_0 \frac{1+e^{-j(\pi+e^{j\frac{\pi}{4}})}e^{-j\sqrt{\frac{8\pi^3 cR_H}{s}}}}{1-e^{-j(\pi+e^{j\frac{\pi}{4}})}e^{j\sqrt{-\frac{8\pi^3 cR_H}{s}}}} \\ \mathcal{Z}_L(s) &= z_0 \frac{\coth(-\frac{j}{2}(\pi+e^{j\frac{\pi}{4}}) - j\sqrt{\frac{2\pi^3 cR_H}{s}})}{j} e^{j\pi} \end{aligned} \tag{4.19}$$

$$\mathcal{Z}_L(s) = z_0 e^{-j\frac{\pi}{2}} \coth\left(\frac{j}{2}(\pi + e^{j\frac{\pi}{4}}) + j\sqrt{\frac{2\pi^3 cR_H}{s}}\right). \tag{4.20}$$

The complex impedance is also complex analytic and therefore has a causal inverse Laplace transform $\zeta_L(t) \leftrightarrow \mathcal{Z}_L(s)$.

CHAPTER 5

INVERSE

In this section we attempt a few directions of deriving the area function from our $\Gamma_L(s)$ derived in Eq. 4.18.

5.1 Quadratic Formula Inverse

Here, we can apply the approach of Eq. 3.36 for the Rydberg energy levels. We can put the phase of $\Gamma(s)$ into Eq. 4.1 and find

$$\varphi(\omega) = \pi + \sqrt{\frac{8\pi^3 c R_H}{\omega}}. \tag{5.1}$$

Applying the boundary condition of Eq. 3.23 we find

$$\begin{aligned} k(\omega)L &= -\pi - \sqrt{\frac{8\pi^3 c R_H}{\omega}} \\ k(\omega) &= -\frac{\pi}{L} - \frac{2\pi}{L}\sqrt{\frac{2\pi c R_H}{\omega}}. \end{aligned} \tag{5.2}$$

Matching a, b, d from the horn equation we arrive at

$$\frac{\sqrt{4ad - b^2}}{2a} = -\frac{\pi}{L} - \frac{2\pi}{L}\sqrt{\frac{2\pi c R_H}{\omega}}. \tag{5.3}$$

Assuming $P(x) = P_0 e^{j\omega t - \kappa x}$ and $\omega, A(x)$ have no κ dependence we have the constraints $a = 1, d = \frac{\omega^2}{c^2}$. Solving for the remaining unkown, b, we have

$$\begin{aligned} \frac{\sqrt{4\frac{\omega^2}{c^2} - b^2}}{2} &= -\frac{\pi}{L} - \frac{2\pi}{L}\sqrt{\frac{2\pi c R_H}{\omega}} \\ b^2 = 4\frac{\omega^2}{c^2} &- 4\frac{\pi^2}{L^2}\left(1 + 2\sqrt{\frac{2\pi c R_H}{\omega}}\right)^2. \end{aligned} \tag{5.4}$$

This answer is unsatisfactory because it gives $\frac{1}{A(x)}\frac{\partial A(x)}{\partial x}$ ω dependence which violates our assumption that $A(x)$ have no κ dependence.[1] Therefore, Eq. 5.4 shows that the Webster's horn area function has no closed form area function.

5.2 Youla Inverse Technique

In Youla's paper [You64], it is shown that given $\Gamma_L(s)$ and a few constants we can synthesize an approximate solution to a horn waveguide as in Webster's horn equation.[2] We setup the technique here but the application is beyond the scope of this senior thesis. To utilize this technique we need to define $H(s)$ as the Laplace transform of $A(x)$

$$H(s) = \int_0^L e^{-sx} A(x) dx \tag{5.5}$$

where L is the length of the waveguide. From [You64] Eq. 90,

$$H(s) = k\frac{r(s/2) - e^{-sL}\Gamma_L(s/2)}{1 - e^{-sL}r(s/2)} \tag{5.6}$$

[1] κ is frequency dependent and ω and κ are not orthogonal.

[2] In Youla'a paper the area function is given by the *log-line taper*.

where $r(s)$ is a Volterra series solution for the first approximation to the input reflection coefficient of a lossless line matched at the input and shorted at the output,[3]

$$r(s) = \frac{k\Gamma_L(s)e^{-2sL} + \int_0^L e^{-sx} A(x)dx}{k + \Gamma_L(s)e^{-2sL} \int_0^L e^{-sx} A(x)dx}. \tag{5.7}$$

[3]From Youla[You64], we replaced $s_{11}(p)$ by $r(s)$ in order to keep s consistent as $\sigma + j\omega$.

CHAPTER 6

CONCLUSION

We have shown the area function of fixed length Webster's horn for the energy levels of hydrogen has no closed form solution, Eq. 5.4. After discovering this result, we have setup the method of D. C. Youla [You64] in Section 5.2, which guarantees an iterative volterra series solution. If continuing the work of 5.2 leads to an unsatisfactory result, challenging the assumptions of the Webster's horn equation derivation in appendix A by investigating the semi-infinite horn or alternate κ dependence could lead to a resolution. Another direction is to apply the technique of [Sal46] in order vary the area function of the 3D conical horn, Eq. 1.4, in order to fit the Coulomb potential.

APPENDIX A

WEBSTER'S HORN EQUATION DERIVATION

The acoustic wave equation comes from the stiffness of air and its mass.[1] Starting with these quantities, we find the conservation of momentum density to be

$$-\nabla p(x,t) = \rho_0 \frac{\partial}{\partial t} u(x,t) \tag{A.1}$$

and conservation of mass density to be

$$-\nabla \cdot u = \frac{1}{\eta_0 P_0} \frac{\partial}{\partial t} u(x,t). \tag{A.2}$$

Conservation of momentum: If we integrate the normal component of Eq. A.1 over the iso-pressure wave front $\mathcal{S}$ we have

$$-\int_{\mathcal{S}} \nabla p(\mathbf{x},t) \cdot d\mathbf{A} = \rho_0 \frac{\partial}{\partial t} \int_{\mathcal{S}} \mathbf{u}(\mathbf{x},t) \cdot d\mathbf{A}. \tag{A.3}$$

Figure A.1 shows this geometry where the iso-pressure surface is given by $A(x)$. Now we define the *average pressure* on the iso-pressure surface $\mathcal{S}$ as

$$\rho(x,t) \equiv \frac{1}{A(x)} \int_{\mathcal{S}} p(x,t) \hat{\mathbf{n}} \cdot d\mathbf{A} \tag{A.4}$$

and the *volume velocity* as

$$\nu(x,t) \equiv \int_{\mathcal{S}} \mathbf{u}(\mathbf{x},t) \cdot d\mathbf{A}. \tag{A.5}$$

[1] This derivation mirrors that of Allen's paper [All].

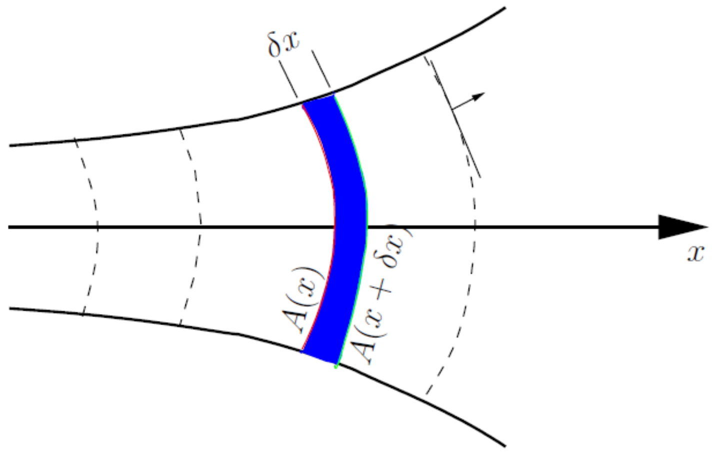

Figure A.1: Wavefront geometry

Thus the integral in Eq. A.3 becomes

$$\frac{\partial}{\partial x}\rho(x,t) = -\frac{\rho_0}{A(x)}\frac{\partial}{\partial t}\nu(x,t). \tag{A.6}$$

Conservation of mass: Integrating Eq. A.2 over the volume $\mathcal{V}$ of Fig. A.1 gives

$$-\int_{\mathcal{V}} \nabla \cdot \mathbf{u} dV = \frac{1}{\eta_0 P_0}\frac{\partial}{\partial t}\int_{\mathcal{V}} p(\mathbf{x},t)dV. \tag{A.7}$$

Applying Gauss' law to the left-hand side and using the definition of ρ in the limit $\delta x \to 0$ gives

$$\frac{\partial}{\partial x}\nu(x,t) = -\frac{A(x)}{\eta_0\rho_0}\frac{\partial}{\partial t}\rho(x,t). \tag{A.8}$$

Combination into Webster's Horn Equation: Taking $\frac{\partial}{\partial x}$ of the momentum equation, Eq. A.6, and $\frac{\partial}{\partial t}$ of the mass equation, Eq. A.8, gives Webster's horn equation:

$$
\begin{aligned}
\frac{1}{A(x)}\partial_x(A(x)\rho_x) &= \frac{\rho_0}{P_0\eta_0}\frac{\partial^2\rho}{\partial t^2} \\
\frac{\partial^2\rho}{\partial x^2} + \frac{1}{A(x)}\frac{\partial A(x)}{\partial x}\frac{\partial\rho}{\partial x} &= \frac{1}{c^2}\frac{\partial^2\rho}{\partial t^2}.
\end{aligned}
\tag{A.9}
$$

REFERENCES

[All] Jont Allen. The Sturm-Liouville Webster horn equation. Unpublished.

[atUoNL] Astronomy Education at the University of Nebraska-Lincoln. Transitions. website `http://astro.unl.edu/naap/hydrogen/transitions.html`.

[Boh13] N. Bohr. On the constitution of atoms and molecules. *Philos. Mag.*, 26:8, 1913.

[BSI94] David Berners and Julius O. Smith III. On the use of Schrodinger's equation in the analytic determination of horn reflectance. In *Arhus, Denmark. Computer Music Association*, pages 419–422, 1994.

[Che] Weng Cho Chew. Quantum mechanics made simple. `http://wcchew.ece.illinois.edu/chew/course/QMALL20121005.pdf`.

[DC12] Dimitri M. Donskoy and Benjamin A. Cray. Acoustic particle velocity horns. *J. Acoust. Soc. Am.*, pages 3883–3890, 2012.

[Jon] Timothy Jones. The Legendre and Laguerre polynomials and the elementary quantum mechanical model of the hydrogen atom.

[Kol] Bjorn Kolbrek. Horn theory: An introduction, part 1. website `http://www.audioXpress.com`.

[Mor48] Philip Morse. *Vibration and Sound*. McGraw-Hill, New York, 1948.

[Ols47] H. F. Olson. *Elements of Acoustical Engineering (2nd Edition)*. D. Van Nostrand Company, 1947.

[Pie81] A. D. Pierce. *Acoustics: An Introduction to Its Physical Principles and Applications*. McGraw-Hill, New York, 1981.

[Ram] Caitlin Jo Ramsey. Hydrogen spectral series plotted on a log scale. website `https://upload.wikimedia.org/wikipedia/commons/2/2d/HydrogenSpectrum.PNG`.

[Sal46] Vincent Salmon. Generalized plane wave horn theory. *J. Acoust. Soc. Am.*, 17(3):200, 1946.

[Sha70] E. Shaw. Acoustic horns with spatially varying density or elasticity. *J. Acoust. Soc. Am.*, pages 830–840, 1970.

[Som49] Arnold Sommerfeld. *Partial Differential Equations in Physics*, pages 200–206. Levant Books, 1949.

[Tow10] John S. Townsend. *Quantum Physics*. University Science Books, 2010.

[Val64] M. E. Van Valkenburg. *Modern Network Synthesis*. John Wiley and Sons, New York, 1964.

[Web19] A. G. Webster. Acoustical impedance, and the theory of horns and of the phonograph. *Proc. Nat. Acad. Sci.*, pages 275–282, 1919.

[You64] D.C. Youla. Analysis and synthesis of arbitrarily terminated lossless nonuniform lines. *IEEE Transactions on Circuit Theory*, pages 363–372, 1964.